



**Title: FORCCHN V2.0: An individual tree-based model for predicting multiscale forest carbon dynamics**

**Authors:** Jing Fang<sup>1,2</sup>, Herman H. Shugart<sup>3</sup>, Feng Liu<sup>1,2</sup>, and Xiaodong Yan<sup>4\*</sup>, Yunkun Song<sup>4</sup>, Fucheng Lv<sup>4</sup>

1. CAS Key Laboratory of Aquatic Botany and Watershed Ecology, Wuhan Botanical Garden, Chinese Academy of Sciences, Wuhan 430074, China
2. Center of Plant Ecology, Core Botanical Gardens, Chinese Academy of Sciences, Wuhan 430074, China
3. Department of Environmental Sciences, University of Virginia, Charlottesville, VA 22904, USA.
4. State Key Laboratory of Earth Surface Processes and Resource Ecology, Beijing Normal University, Beijing 100875, China

Corresponding author: Xiaodong Yan (yxd@bnu.edu.cn)



## 1 **Abstract**

2 Process-based ecological models are essential tools to quantify and predict forest growth and carbon cycle  
3 under the background of climate change. The accurate description of phenology and tree growth processes  
4 enables an improved understanding and predictive modeling of forest dynamics. An individual tree-based  
5 carbon model, FORCCHN2 (FORest ecosystem Carbon budget model for CHiNa Version 2.0), used the  
6 non-structural carbohydrates (NSC) pools to couple tree growth and phenology. This model performed  
7 well in reducing uncertainty in predicting forest carbon fluxes. Here, we describe the framework in detail  
8 and provide the source code of FORCCHN2. We also present a Dynamic Link Library (DLL) package  
9 containing the latest version of the FORCCHN2 model. This package has the advantage of using Fortran  
10 as an interface to make the model runs fast on a daily step, the package also allows the users to call it with  
11 their preferred computer tools (e.g., Matlab, R, Python, *etc.*). FORCCHN2 model can be used directly to  
12 predict the yearly phenology as well as the daily carbon fluxes (including photosynthesis, above- and  
13 belowground autotrophic respiration, and soil heterotrophic respiration) and biomass on plot, regional,  
14 and global scales. As case studies, we provide an example of the FORCCHN2 running, model validations  
15 in 78 forest sites, and an example model application for the carbon dynamics of Northern Hemisphere  
16 forests. We demonstrate the FORCCHN2 model can produce a reasonable agreement with flux  
17 observations. Given the potential importance of the application of this ecological model in many studies,  
18 there is substantial scope for using the FORCCHN2 model in fields as diverse as forest ecology, climate



19 change, and carbon estimations.

20

21 **Keywords:** ecological models, forest ecosystems, carbon cycle, non-structural carbohydrates, individual

22 tree, leaf phenology



## 23 **1. Introduction**

24 Forests contribute an enormous carbon flux to terrestrial ecosystems (Pan et al. 2011, Keenan and  
25 Williams 2018). Thus, accurate estimation and prediction of forest dynamics play an important role in  
26 understanding the carbon cycle in the background of global change (Beer et al. 2010, Harris et al. 2021).  
27 Over past decades, process-based ecological models have often been considered as effective tools for  
28 evaluating forest dynamics at multiple scales (Friedlingstein et al. 2020).

29 Even though the ecological models are widely used in the prediction of forest dynamics, large  
30 uncertainties remain (Huntzinger et al. 2012, Friedlingstein et al. 2020). Some of these uncertainties can  
31 be attributed to the lack of effective phenological parameterization in the models and the neglect of  
32 autumn phenology modeling (Raczka et al. 2013), both of which need to be based on an improved  
33 understanding and coupling of mechanisms regulating forest phenology (Piao et al. 2019). Furthermore,  
34 the previous models assumed that the reserve carbon of trees acts merely as a carbon buffer pool between  
35 sink and source (Schiestl-Aalto et al. 2015). Recent studies considered the stored carbon as the non-  
36 structural carbohydrates (NSC), which may have an active role on tree growth and carbon dynamics  
37 (Martínez-Vilalta et al. 2016, Piper 2020). For example, trees rely on NSC to resume growth after the  
38 non-growing season (Furze et al. 2019). The individual tree-based model, FORCCHN version 2.0  
39 (FORCCHN2), has been developed to treat these considerations by integrating two NSC pools (NSC  
40 active and slow pool) and optimizing phenological parameters (Fang et al. 2020a, Fang et al. 2021).





41 FORCCHN2 has improved performance for predicting forest carbon sinks compared to other models in  
42 North American forests (Fang et al. 2020b).

43 This model provides the temporal predictions of individual tree growth processes as well as the  
44 spatially explicit estimations of carbon dynamics on biomass, photosynthesis, autotrophic respiration, and  
45 heterotrophic respiration (Fang et al. 2020b). The latest version can capture forest carbon dynamics, but  
46 current runs of FORCCHN2 have limitations that prevent a seamless integration of the model into the  
47 data-oriented software environment (e.g., Matlab, R, Python, etc.). FORCCHN2 and its previous versions  
48 are designed originally for the daily calculation of individual trees in a given plot and implemented in  
49 Fortran (Ma et al. 2017, Zhao et al. 2019, Fang et al. 2020a). Fortran ensures the calculation efficiency  
50 and shortens the model runtime, but the model code and the implementation are not designed for the end-  
51 users with appropriate help and instruction files. Moreover, until now, the FORCCHN2 model has only  
52 been validated and applied in North America, and there has been no comprehensive publication describing  
53 the model itself and no global-scale validation using this model.

54 Here, we present a DLL package aimed to provide a flexible and user-friendly interface for  
55 implementing the newest FORCCHN2 model. Meanwhile, we provide the source code and the detailed  
56 description of this model and demonstrates that FORCCHN2 model can predict a realistic and stable  
57 carbon dynamics in the global-scale forests. With the package, users can conveniently run model  
58 predictions on the individual, plot, regional, continental, and global scales according to their computer



59 tools. This package is compiled by Fortran 95 and thus can keep the high calculation efficiency. We also  
60 demonstrate the functionality and example of FORCCHN2 model, perform the model validation at the  
61 carbon flux sites, apply the model on a global scale (i.e. Northern Hemisphere), and provide an open-  
62 access dataset of carbon outputs across the Northern Hemisphere.

63

## 64 **2. FORCCHN2 description**

65 FORCCHN2, an individual tree-based carbon dynamic model, predicts the daily processes of NSC,  
66 photosynthesis, growth, phenology, vegetation (autotrophic) respiration, and soil dynamics in forests (**Fig.**  
67 **1** and **Method S1-S2**). This model is driven by the daily climate data and uses the leaf area index (LAI)  
68 to initialize the vegetation information (i.e., trees' number, DBH, height, and biomass) on a fixed area  
69 (**Method S3**).

70 For an individual tree, the NSC produced by photosynthesis is considered as the substrate supply for  
71 vital activities, such as participating the autotrophic respiration and forming the structural carbon pools  
72 (i.e., leaves, wood, and fine roots) through growth (Sala et al. 2012, Richardson et al. 2013). The NSC  
73 production is limited by external environmental factors (e.g., water, temperature, CO<sub>2</sub>, etc.), and the NSC  
74 consumption for the growth of each structural carbon pool (i.e., leaves, wood, and fine roots) is regulated  
75 by phenology factors and daily climate (Schiestl-Aalto et al. 2015, Delpierre et al. 2019). The phenology  
76 in FORCCHN2 is controlled by heat and chilling. The model divides NSC into an active NSC pool and a



77 slow NSC pool. The active pool provides the essential NSC consumption for daily activities; the slow  
78 pool is an NSC storage pool providing the necessary NSC for requirements when the contemporaneous  
79 active pool is insufficient, such as maintaining vegetation respiration during the non- and early-growing  
80 seasons. These NSC pools allow trees to be dead if the NSC storage drops below zero.

81 Major control equation of each individual tree: Dynamic changes of NSC production, allocation and  
82 consumption drive change in the NSC active pool ( $NSC_{active}$ , kg C) at a daily time step. The NSC slow  
83 pool ( $NSC_{slow}$ , kg C) is defined as the NSC storage pool. The changes in the daily active pool and yearly  
84 slow pool are:

$$\frac{dNSC_{active}}{dt} = \frac{dGPP}{dt} - \sum \frac{dR_j}{dt} - \sum \frac{dR_j^G}{dt} - \sum \frac{dG_j}{dt} \quad (1)$$

$$NSC_{slow}(y) = NSC_{active,y} \quad (2)$$

85 Where  $t$  is the day of the year;  $y$  is the  $y$ th year;  $j$  is each part of the tree (i.e. leaf, fine roots, and wood);  
86 GPP is gross primary productivity (kg C);  $R$  is the maintenance respiration (kg C);  $R^G$  is the growth  
87 respiration (kg C);  $G$  is the carbon demand of growth (kg C);  $NSC_{active,y}$  is the size of NSC active pool at  
88 the end of  $y$ th year (kg C). The NSC active pool is initialized to zero on the first day of the next year. The  
89 calculation of GPP, maintenance respiration, growth respiration, and growth processes can be found in  
90 **Method S1** and **S2**.

91 For the relationship between an individual tree with its neighbors, the model uses a distance-  
92 independent gap model to describe the light competition. To simplify the physiological and ecological



93 parameters, each individual tree is assumed to belong to the plant functional types (PFTs) instead of  
94 specific tree species (**Table S2**). The phenological parameters are parameterized by the local climate and  
95 observed phenological time in the first year (**Eqn S43-S45**). A part of structural carbon pools is then  
96 transferred into the soil pools by litter-fall. The main soil processes in the FORCCHN2 model are soil  
97 organic matter (SOM) decomposition, N mineralization, and water dynamics. According to the attribute,  
98 soil pools include above- and belowground metabolic and structural pools; fine and coarse woody litter  
99 pools; active, slow, and resistant SOM pools (**Table S4**). Except for these pools, the soil nitrogen pool  
100 also includes the inorganic nitrogen pool.

101 After each time step, the predicted vegetation and soil statements are converted into output variables  
102 such as biomass and carbon fluxes. The carbon fluxes of plot scale include GPP (kg C m<sup>-2</sup>), net primary  
103 productivity (NPP, kg C m<sup>-2</sup>), and net ecosystem productivity (NEP, kg C m<sup>-2</sup>). The NPP of a given plot  
104 at the daily step was determined by the GPP, R (kg C m<sup>-2</sup>), R<sup>G</sup> (kg C m<sup>-2</sup>). The NEP of a given plot at the  
105 daily step was determined by the GPP, R, R<sup>G</sup>, and soil respiration (R<sub>s</sub>, kg C m<sup>-2</sup>):

$$\frac{dNPP}{dt} = \sum \frac{dGPP_n}{dt} - \sum \frac{dR_n}{dt} - \sum \frac{dR_n^G}{dt} \quad (3)$$

$$\frac{dNEP}{dt} = \frac{dNPP}{dt} - \frac{dR_s}{dt} \quad (4)$$

106 Where  $n$  is the  $n$ th tree of the plot.

107 The more detailed description, including inputs, outputs, calculation processes, and parameter sets  
108 of FORCCHN2, can be found in **Table 1**, **Method S1-S3**, and **Table S2-S5**.



109

### 110 **3. Example runs**

111 Here, we provide an integrated DLL package ('FORCCHN2.dll') to simplify the usage of the  
112 FORCCHN2 model. This file is highly flexible and it allows users to adapt model runs using with their  
113 own computer language (e.g., Matlab, R, Fortran, Python, etc.). Except for the model inputs, using only  
114 one command can call the calculation of the model. We provide users with 32- and 64-bit DLL packages  
115 to choose the most suitable version.

116 We took the Harvard Forest (a deciduous broadleaf forest in the eastern United States) and used  
117 Matlab as an example run to demonstrate the functionality of the FORCCHN2 model (the code of example  
118 also can be accessed via [https://github.com/JingF1/FORCCHN2\\_model.git](https://github.com/JingF1/FORCCHN2_model.git)). First, installed and loaded  
119 the package:

```
120 >>name1=('XXX');%load path of the FORCCHN2 DLL package  
121 >>name2=[name1,'FORCCHN2_64.dll']; %input 64-bit or 32-bit DLL file  
122 >>name3=[name1,'FORCCHN2.h'];%input header file  
123 >>loadlibrary(name2,name3);%load the DLL package
```

124 Then, we inputted the data of Harvard Forest during 1991-2012. The inputs included the year  
125 information, the initialization data (i.e., geography, vegetation, and soil data), and the driven data (i.e.,  
126 climate data). The more detailed information and format of these input data can be found in the example



127 code ('FORCCHN2\_run\_example.m').

128 After inputting all data, we predicted the dynamics of this forest for a period of 22 years. We can  
129 choose four output results of the FORCCHN2:

```
130 >>[fj,ycx,dayout,yearout]=calllib('FORCCHN2_64','forcchn2',fj,ycx,dayout,yearout,ntrees,ny0,ny,nday  
131 s,lat,lon,ele,tmax,tmin,tmean,pho,prec,ra,rh,wind,sfc,pwp,vw,sc0,sn0,silt,sand,class1,evergr0,deci0,lai0,  
132 co2);% run model with DLL file  
133 >>unloadlibrary FORCCHN2; %unload the DLL package
```

134 Where the outputs included: 'fj' was the phenology dates, which included the start time of leaf  
135 growth (SOS) and the end time of leaf growth (EOS); 'ycx' was the allocation parameter of each soil pool,  
136 which can be used as input instead of the initial soil allocation parameters; 'dayout' was the daily carbon  
137 dynamics, which included above- and belowground biomass, gross primary productivity (GPP), above-  
138 and belowground respiration, soil heterotrophic respiration, litter-fall biomass, and soil carbon; 'yearout'  
139 was the yearly carbon dynamics.

140

#### 141 **4. External validation**

142 The comparison between model simulations and external observations was considered as the rigorous  
143 model test (Houlahan et al. 2017). Among the various observation methods, the eddy-covariance (EC)  
144 technique can provide high-frequency and accurate measurements of relevant data (Keenan and Williams



145 2018). The FLUXNET2015 dataset (Pastorello et al. 2020, <https://fluxnet.org/>) from the EC tower was  
146 an ideal dataset to validate the FORCCHN2 model in predicting carbon flux dynamics. This dataset was  
147 developed by using the EC (Eddy Correlation) technique to measure the net ecosystem CO<sub>2</sub> exchange  
148 (NEE, which equaled to the negative of NEP) directly in the footprint of the EC tower. The night-time  
149 NEE was considered as the Ecosystem Respiration (ER). The relation between ER and temperature was  
150 applied to extrapolate the day-time ER (Reichstein et al. 2005). ER equaled the sum of vegetation  
151 autotrophic respiration and soil heterotrophic respiration. The vegetation GPP was estimated by the day-  
152 time NEE and ER (i.e.,  $GPP=ER-NEE$ ) (Lasslop et al. 2010). Due to the different phenological phasing  
153 in the Northern and Southern Hemisphere, our predictions focused on the Northern Hemisphere. We chose  
154 the 78 active forest sites with continuous daily observations in the Northern Hemisphere (i.e., a total of  
155 232664 observations). These sites covered the most forest types, including the evergreen broadleaf forest  
156 (EBF), evergreen needleleaf forest (ENF), deciduous broadleaf forest (DBF), and mixed forest (MF). The  
157 distribution and information of all sites were shown in **Fig. S1** and **Table S1**.

158 We predicted the daily carbon flux in the 78 forest sites and then validated the predictions with the  
159 observations. As the detailed performance, **Fig. 2** showed the direct daily comparison between predictions  
160 and observations. Overall, the model had the best performance in capturing GPP dynamics, followed by  
161 ER and NEP. In the FORCCHN2 model, we used the phenology model and the optimized phenological  
162 parameters to predict the leaf growth, which could improve the predicted performance of GPP (Fang et



163 al. 2020b). We did the statistics for the results in all sites. The validation statistics included the correlation  
164 coefficient ( $R$ ), model efficiency ( $E$ ), root mean square error ( $RMSE$ ), mean absolute error ( $MAE$ ), and  
165 bias ( $Bias$ ). Each site had one group of statistics. **Fig. 3** showed that the FORCCHN2 model could  
166 reproduce the daily dynamics of the carbon flux in all sites, particularly for predicting daily GPP (median  
167 of all sites:  $R=0.86$ ,  $E=0.62$ ,  $RMSE=2.29$  g C m<sup>-2</sup> d<sup>-1</sup>,  $MAE=1.61$  g C m<sup>-2</sup> d<sup>-1</sup>). The predicted ER performed  
168 lower than GPP, but showed a high correlation with the observed ER (median:  $R=0.83$ ,  $E=0.25$ ,  
169  $RMSE=1.46$  g C m<sup>-2</sup> d<sup>-1</sup>,  $MAE=1.04$  g C m<sup>-2</sup> d<sup>-1</sup>). NEP results had the lowest performance in all flux  
170 variables (median:  $R=0.61$ ,  $E=-0.16$ ,  $RMSE=1.91$  g C m<sup>-2</sup> d<sup>-1</sup>,  $MAE=1.43$  g C m<sup>-2</sup> d<sup>-1</sup>). The highest  
171 uncertainty in predicting NEP maybe because of the compounding effect of GPP and ER errors (Balzarolo  
172 et al. 2014). In terms of bias, FORCCHN2 overestimated the GPP and ER (median:  $Bias=0.49$  and  $0.56$   
173 g C m<sup>-2</sup> d<sup>-1</sup>, respectively) but slightly underestimated the NEP (median:  $Bias=-0.14$  g C m<sup>-2</sup> d<sup>-1</sup>). For the  
174 different forest types, the predictions presented well in DBF and MF ( $R=0.84$  and  $0.57$ ,  $E=0.53$  and  $0.64$ ,  
175 respectively), whereas the lowest performance was found in EBF ( $R=0.61$ ,  $E=0.31$ ). These results were  
176 consistent with the previous studies: EBF revealed subtle changes in the leaf phenology and thus increased  
177 the difficulty in modeling photosynthesis (i.e., GPP) (Raczka et al. 2013, Yuan et al. 2014, Piao et al.  
178 2019).

179

## 180 **5. Applications in the Northern Hemisphere**





181 As a case application on large scale, we predicted the carbon dynamics in the Northern Hemisphere forests  
182 during 1980-2016 (spatial resolution: 0.5×0.5 degree). For the Hemisphere, we used the Simple Biosphere  
183 (SiB) model of International Satellite Land Surface Climatology Project (ISLSCP II) to represent forest  
184 types (**Fig. S1**, [https://daac.ornl.gov/ISLSCP\\_II](https://daac.ornl.gov/ISLSCP_II)) (Friedl et al. 2010). The climate data were from the daily  
185 analysis of ERA5 in the European Centre for Medium-range Weather Forecasts (ECMWF) dataset  
186 (Hersbach et al. 2020). Soil data were taken from the Harmonized World Soil Database (HWSD) V1.2  
187 ([http://www.fao.org/soils-porta l/soil-survey/soil-mapsand-datab ases/](http://www.fao.org/soils-porta-l/soil-survey/soil-mapsand-databases/)).

188 **Fig. 4** reported the spatial distribution of 37-year averaged GPP, above- and belowground autotrophic  
189 respiration, soil heterotrophic respiration, net primary productivity (NPP), and net ecosystem productivity  
190 (NEP) for forest area. All results showed a similar spatial pattern with the largest fluxes occurring around  
191 the equator, such as the northern part of the Amazon and Central African tropical rainforests; secondly,  
192 the monsoonal subtropical regions such as South Asia and eastern North America showed the large fluxes;  
193 the northern forests near the Arctic Circle had the smallest fluxes. Overall, our predictions demonstrated  
194 that the forests in Northern Hemisphere had a huge carbon sink potential by the vegetation (i.e.,  
195  $NPP=16.76 \text{ Pg C year}^{-1}$  or  $61.45 \text{ Gt CO}_2 \text{ year}^{-1}$ ) and the total ecosystem ( $NEP=3.19 \text{ Pg C year}^{-1}$  or  $11.70$   
196  $\text{Gt CO}_2 \text{ year}^{-1}$ ) during 1980-2016, which was within the range of the newest estimation of forest carbon  
197 sinks (Harris et al. 2021). The predicted carbon results including the variables of ‘dayout’ and ‘yearout’  
198 in this case (i.e., Northern Hemisphere forests) were deposited at an open-access repository (Fang 2022:



199 <https://doi.org/10.6084/m9.figshare.18318722.v1>).

200

## 201 **6. Conclusions**

202 We developed the FORCCHN2 model and designed the corresponding DLL package with the intention  
203 to simplify the input and processing of the model and make it more accessible to ecologists interested in  
204 the forest ecosystem, climate change, carbon cycle, and modeling. This package provides convenient  
205 access and allows high computational efficiency with the Fortran-language-based model predicting the  
206 daily dynamics of individual trees. With this new package, we have demonstrated the workflow, functions,  
207 and applications of the FORCCHN2 model.

208 In addition, the FORCCHN2 model was tested at 78 flux sites, and then it was applied in predicting  
209 the carbon dynamics in the whole Northern Hemisphere forests (1980-2016). Our assessment indicated  
210 that FORCCHN2 was able to predict the satisfactory carbon dynamics. While we provided publicly  
211 available data in the Northern Hemisphere with 0.5 degrees, our hope is that end-users can offer a wide  
212 range of applications and analyses of the FORCCHN2 model, such as providing the new dataset with  
213 finer resolution and estimating future changes of forest carbon fluxes. We are also open to further  
214 suggestions on enhanced functions that ecologists may find helpful in the subsequent model versions.

215

## 216 **Acknowledgements**



217 This study was supported by the National Natural Science Foundation of China (32101349, 32171599).

218 This study also was supported by the Key Program of the National Natural Science Foundation of China  
219 (32130069) and the National Key Research and Development Program of China (grant  
220 2019YFC0606904).

221

### 222 **Authors' contributions**

223 JF planned the project. XY and JF conducted the modeling. XY, JF, YS, and FL contributed to data  
224 collection. HHS and JF contributed to data analysis and interpretation of the results. HHS, FL and JF took  
225 the lead in writing the manuscript. JF feedback and approval from co-authors. The authors have no  
226 conflicts of interest to report.

227

### 228 **Data availability statement**

229 The source code, instructions, and example run, together with FORCCHN2 DLL package are publicly  
230 available via <https://doi.org/10.5281/zenodo.6351153> (Fang et al. 2022). The datasets predicted by  
231 FORCCHN2 model include the 37-year (1980-2016) GPP, above- and belowground autotrophic  
232 respiration, soil heterotrophic respiration for Northern Hemisphere forests ( $0.5^{\circ} \times 0.5^{\circ}$ ) are publicly  
233 available via <https://doi.org/10.6084/m9.figshare.18318722.v1> (Fang 2022).

234



## 235 Reference

- 236 Balzarolo, M., S. Boussetta, G. Balsamo, A. Beljaars, F. Maignan, J. C. Calvet, S. Lafont, A. Barbu, B. Poulter, F. Chevallier,  
237 C. Szczypta, and D. Papale. 2014. Evaluating the potential of large-scale simulations to predict carbon fluxes  
238 of terrestrial ecosystems over a European Eddy Covariance network. *Biogeosciences* **11**:2661-2678.
- 239 Beer, C., M. Reichstein, E. Tomelleri, P. Ciais, M. Jung, N. Carvalhais, C. Rödenbeck, M. A. Arain, D. Baldocchi, B. Bonan  
240 Gordon, A. Bondeau, A. Cescatti, G. Lasslop, A. Lindroth, M. Lomas, S. Luysaert, H. Margolis, W. Oleson Keith,  
241 O. Roupsard, E. Veenendaal, N. Viovy, C. Williams, F. I. Woodward, and D. Papale. 2010. Terrestrial Gross  
242 Carbon Dioxide Uptake: Global Distribution and Covariation with Climate. *Science* **329**:834-838.
- 243 Delpierre, N., S. Lireux, F. Hartig, J. J. Camarero, A. Cheaib, K. Čufar, H. Cuny, A. Deslauriers, P. Fonti, J. Gričar, J.-G.  
244 Huang, C. Krause, G. Liu, M. de Luis, H. Mäkinen, E. M. del Castillo, H. Morin, P. Nöjd, W. Oberhuber, P. Prislan,  
245 S. Rossi, S. M. Saderi, V. Treml, H. Vavrick, and C. B. K. Rathgeber. 2019. Chilling and forcing temperatures  
246 interact to predict the onset of wood formation in Northern Hemisphere conifers. *Global Change Biology*  
247 **25**:1089-1105.
- 248 Fang, J. 2022. Daily and annual carbon flux predicted by FORCCHN2 model. figshare.
- 249 Fang, J., H. H. Shugart, Liu, F., Yan X., Song, Y., and Lv, F. 2022. FORCCHN2 model (v2.0.1). Zenodo.  
250 <https://doi.org/10.5281/zenodo.6351153>
- 251 Fang, J., J. A. Lutz, H. H. Shugart, and Yan X. 2020a. A physiological model for predicting dynamics of tree stem-wood  
252 non-structural carbohydrates. *Journal of Ecology* **108**:702-718.
- 253 Fang, J., J. A. Lutz, H. H. Shugart, Yan X., W. Xie, and F. Liu. 2021. Improving intra- and inter-annual GPP predictions  
254 by using individual tree inventories and leaf growth dynamics. *Journal of Applied Ecology* **58**:2315-2328.
- 255 Fang, J., J. A. Lutz, L. Wang, H. H. Shugart, and Yan X. 2020b. Using climate-driven leaf phenology and growth to  
256 improve predictions of gross primary productivity in North American forests. *Global Change Biology* **26**:6974-  
257 6988.
- 258 Friedl, M. A., A. H. Strahler, and J. Hodges. 2010. ISLSCP II MODIS (Collection 4) IGBP Land Cover, 2000-2001. ORNL  
259 Distributed Active Archive Center.
- 260 Friedlingstein, P., M. O'Sullivan, M. W. Jones, R. M. Andrew, J. Hauck, A. Olsen, G. P. Peters, W. Peters, J. Pongratz, S.  
261 Sitch, C. Le Quéré, J. G. Canadell, P. Ciais, R. B. Jackson, S. Alin, L. E. O. C. Aragão, A. Arneeth, V. Arora, N. R.  
262 Bates, M. Becker, A. Benoit-Cattin, H. C. Bittig, L. Bopp, S. Bultan, N. Chandra, F. Chevallier, L. P. Chini, W. Evans,  
263 L. Florentie, P. M. Forster, T. Gasser, M. Gehlen, D. Gilfillan, T. Gkritzalis, L. Gregor, N. Gruber, I. Harris, K.  
264 Hartung, V. Haverd, R. A. Houghton, T. Ilyina, A. K. Jain, E. Joetzjer, K. Kadono, E. Kato, V. Kitidis, J. I. Korsbakken,  
265 P. Landschützer, N. Lefèvre, A. Lenton, S. Lienert, Z. Liu, D. Lombardozzi, G. Marland, N. Metzl, D. R. Munro, J.  
266 E. M. S. Nabel, S. I. Nakaoka, Y. Niwa, K. O'Brien, T. Ono, P. I. Palmer, D. Pierrot, B. Poulter, L. Resplandy, E.  
267 Robertson, C. Rödenbeck, J. Schwinger, R. Séférian, I. Skjelvan, A. J. P. Smith, A. J. Sutton, T. Tanhua, P. P. Tans,  
268 H. Tian, B. Tilbrook, G. van der Werf, N. Vuichard, A. P. Walker, R. Wanninkhof, A. J. Watson, D. Willis, A. J.  
269 Wiltshire, W. Yuan, X. Yue, and S. Zaehle. 2020. Global Carbon Budget 2020. *Earth Syst. Sci. Data* **12**:3269-  
270 3340.



- 271 Furze, M. E., B. A. Huggett, D. M. Aubrecht, C. D. Stolz, M. S. Carbone, and A. D. Richardson. 2019. Whole-tree  
272 nonstructural carbohydrate storage and seasonal dynamics in five temperate species. *New Phytologist*  
273 **221**:1466-1477.
- 274 Harris, N. L., D. A. Gibbs, A. Baccini, R. A. Birdsey, S. de Bruin, M. Farina, L. Fatoyinbo, M. C. Hansen, M. Herold, R. A.  
275 Houghton, P. V. Potapov, D. R. Suarez, R. M. Roman-Cuesta, S. S. Saatchi, C. M. Slay, S. A. Turubanova, and A.  
276 Tyukavina. 2021. Global maps of twenty-first century forest carbon fluxes. *Nature Climate Change* **11**:234-240.
- 277 Hersbach, H., B. Bell, P. Berrisford, S. Hirahara, A. Horányi, J. Muñoz-Sabater, J. Nicolas, C. Peubey, R. Radu, D. Schepers,  
278 A. Simmons, C. Soci, S. Abdalla, X. Abellan, G. Balsamo, P. Bechtold, G. Biavati, J. Bidlot, M. Bonavita, G. De  
279 Chiara, P. Dahlgren, D. Dee, M. Diamantakis, R. Dragani, J. Flemming, R. Forbes, M. Fuentes, A. Geer, L.  
280 Haimberger, S. Healy, R. J. Hogan, E. Hólm, M. Janisková, S. Keeley, P. Laloyaux, P. Lopez, C. Lupu, G. Radnoti,  
281 P. de Rosnay, I. Rozum, F. Vamborg, S. Villaume, and J.-N. Thépaut. 2020. The ERA5 global reanalysis. *Quarterly*  
282 *Journal of the Royal Meteorological Society* **146**:1999-2049.
- 283 Houlahan, J. E., S. T. McKinney, T. M. Anderson, and B. J. McGill. 2017. The priority of prediction in ecological  
284 understanding. *Oikos* **126**:1-7.
- 285 Huntzinger, D. N., W. M. Post, Y. Wei, A. M. Michalak, T. O. West, A. R. Jacobson, I. T. Baker, J. M. Chen, K. J. Davis, D. J.  
286 Hayes, F. M. Hoffman, A. K. Jain, S. Liu, A. D. McGuire, R. P. Neilson, C. Potter, B. Poulter, D. Price, B. M. Raczka,  
287 H. Q. Tian, P. Thornton, E. Tomelleri, N. Viovy, J. Xiao, W. Yuan, N. Zeng, M. Zhao, and R. Cook. 2012. North  
288 American Carbon Program (NACP) regional interim synthesis: Terrestrial biospheric model intercomparison.  
289 *Ecological Modelling* **232**:144-157.
- 290 Keenan, T. F., and C. A. Williams. 2018. The Terrestrial Carbon Sink. *Annual Review of Environment and Resources*  
291 **43**:219-243.
- 292 Lasslop, G., M. Reichstein, D. Papale, A. D. Richardson, A. Arneeth, A. Barr, P. Stoy, and G. Wohlfahrt. 2010. Separation  
293 of net ecosystem exchange into assimilation and respiration using a light response curve approach: critical  
294 issues and global evaluation. *Global Change Biology* **16**:187-208.
- 295 Ma, J., H. H. Shugart, X. Yan, C. Cao, S. Wu, and J. Fang. 2017. Evaluating carbon fluxes of global forest ecosystems by  
296 using an individual tree-based model FORCCHN. *Science of The Total Environment* **586**:939-951.
- 297 Martínez-Vilalta, J., A. Sala, D. Asensio, L. Galiano, G. Hoch, S. Palacio, F. I. Piper, and F. Lloret. 2016. Dynamics of non-  
298 structural carbohydrates in terrestrial plants: a global synthesis. *Ecological Monographs* **86**:495-516.
- 299 Pan, Y., A. Birdsey Richard, J. Fang, R. Houghton, E. Kauppi Pekka, A. Kurz Werner, L. Phillips Oliver, A. Shvidenko, L.  
300 Lewis Simon, G. Canadell Josep, P. Ciais, B. Jackson Robert, W. Pacala Stephen, A. D. McGuire, S. Piao, A.  
301 Rautiainen, S. Sitch, and D. Hayes. 2011. A Large and Persistent Carbon Sink in the World's Forests. *Science*  
302 **333**:988-993.
- 303 Pastorello, G., C. Trotta, E. Canfora, H. Chu, D. Christianson, Y.-W. Cheah, ... and D. Papale. 2020. The FLUXNET2015  
304 dataset and the ONEFlux processing pipeline for eddy covariance data. *Scientific data* **7**:225.
- 305 Piao, S., Q. Liu, A. Chen, I. A. Janssens, Y. Fu, J. Dai, L. Liu, X. Lian, M. Shen, and X. Zhu. 2019. Plant phenology and  
306 global climate change: Current progresses and challenges. *Global Change Biology* **25**:1922-1940.
- 307 Piper, F. I. 2020. Decoupling between growth rate and storage remobilization in broadleaf temperate tree species.



- 308 Functional ecology **34**:1180-1192.
- 309 Raczka, B. M., K. J. Davis, D. Huntzinger, R. P. Neilson, B. Poulter, A. D. Richardson, J. Xiao, I. Baker, P. Ciais, T. F. Keenan,  
310 B. Law, W. M. Post, D. Ricciuto, K. Schaefer, H. Tian, E. Tomelleri, H. Verbeeck, and N. Viovy. 2013. Evaluation  
311 of continental carbon cycle simulations with North American flux tower observations. *Ecological Monographs*  
312 **83**:531-556.
- 313 Reichstein, M., E. Falge, D. Baldocchi, D. Papale, M. Aubinet, P. Berbigier, C. Bernhofer, N. Buchmann, T. Gilmanov, A.  
314 Granier, T. Grünwald, K. Havránková, H. Ilvesniemi, D. Janous, A. Knohl, T. Laurila, A. Lohila, D. Loustau, G.  
315 Matteucci, T. Meyers, F. Miglietta, J.-M. Ourcival, J. Pumpanen, S. Rambal, E. Rotenberg, M. Sanz, J. Tenhunen,  
316 G. Seufert, F. Vaccari, T. Vesala, D. Yakir, and R. Valentini. 2005. On the separation of net ecosystem exchange  
317 into assimilation and ecosystem respiration: review and improved algorithm. *Global Change Biology* **11**:1424-  
318 1439.
- 319 Richardson, A. D., M. S. Carbone, T. F. Keenan, C. I. Czimczik, D. Y. Hollinger, P. Murakami, P. G. Schaberg, and X. Xu.  
320 2013. Seasonal dynamics and age of stemwood nonstructural carbohydrates in temperate forest trees. *New*  
321 *Phytologist* **197**:850-861.
- 322 Sala, A., D. R. Woodruff, and F. C. Meinzer. 2012. Carbon dynamics in trees: feast or famine? *Tree physiology* **32**:764-  
323 775.
- 324 Schiestl-Aalto, P., L. Kulmala, H. Mäkinen, E. Nikinmaa, and A. Mäkelä. 2015. CASSIA – a dynamic model for predicting  
325 intra-annual sink demand and interannual growth variation in Scots pine. *New Phytologist* **206**:647-659.
- 326 Yuan, W., W. Cai, J. Xia, J. Chen, S. Liu, W. Dong, L. Merbold, B. Law, A. Arain, J. Beringer, C. Bernhofer, A. Black, P. D.  
327 Blanken, A. Cescatti, Y. Chen, L. Francois, D. Gianelle, I. A. Janssens, M. Jung, T. Kato, G. Kiely, D. Liu, B. Marcolla,  
328 L. Montagnani, A. Raschi, O. Roupsard, A. Varlagin, and G. Wohlfahrt. 2014. Global comparison of light use  
329 efficiency models for simulating terrestrial vegetation gross primary production based on the LaThuile  
330 database. *Agricultural and Forest Meteorology* **192-193**:108-120.
- 331 Zhao, J., J. Ma, and Y. Zhu. 2019. Evaluating impacts of climate change on net ecosystem productivity (NEP) of global  
332 different forest types based on an individual tree-based model FORCCHN and remote sensing. *Global and*  
333 *Planetary Change* **182**:103010.



**Table 1.** Description of functions and variables in the FORCCHN2 model. A detailed explanation of functions and variables can be found in the FORCCHN2 DLL package documentation. SOS: the start time of leaf growth; EOS: the end time of leaf growth; DOY: day of the year; GPP: gross primary productivity.

Model functions and variables	Description
Time step	Daily and yearly
Initialization data (inputs)	<p><b>Vegetation:</b> maximum LAI (<math>\text{m}^2 \text{m}^{-2}</math>), forest types, SOS dates (DOY), EOS dates (DOY)</p> <p><b>Soil:</b> field capacity (cm), permanent wilting point (cm), soil volume weight (<math>\text{kg m}^{-3}</math>), total organic carbon (<math>\text{kg C m}^{-2}</math>), total nitrogen (<math>\text{kg C m}^{-2}</math>), silt percent (%), sand percent (%)</p> <p><b>Geography:</b> latitude (<math>^{\circ}</math>), longitude (<math>^{\circ}</math>), elevation (m)</p>
Driven data (inputs)	<p><b>Daily climate:</b> Mean temperature (<math>^{\circ}\text{C}</math>), maximum temperature (<math>^{\circ}\text{C}</math>), minimum temperature (<math>^{\circ}\text{C}</math>), air pressure (hPa), wind (<math>\text{m s}^{-1}</math>), relative humidity (%), precipitation (mm), shortwave radiation (<math>\text{W m}^{-2}</math>), <math>\text{CO}_2</math> concentration (ppm)</p>



---

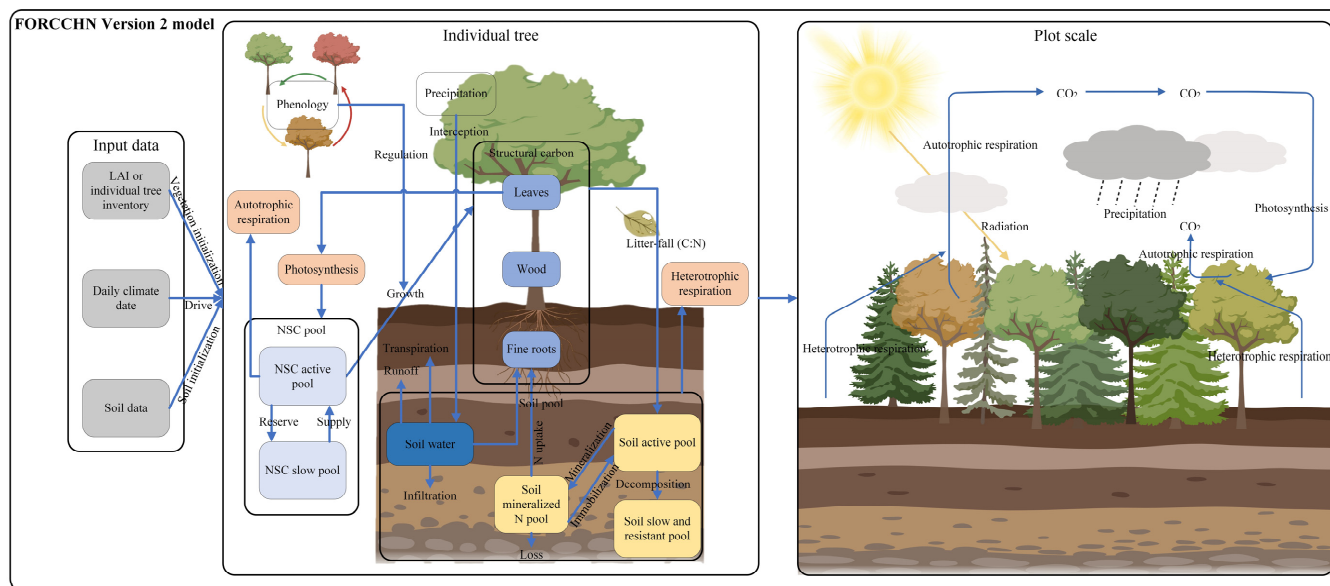
## Outputs

**Daily:** aboveground vegetation biomass ( $\text{kg C m}^{-2}$ ),  
belowground vegetation biomass ( $\text{kg C m}^{-2}$ ), GPP ( $\text{kg C m}^{-2}$ ), aboveground autotrophic respiration ( $\text{kg C m}^{-2}$ ),  
belowground autotrophic respiration ( $\text{kg C m}^{-2}$ ), soil  
heterotrophic respiration ( $\text{kg C m}^{-2}$ ), litter-fall ( $\text{kg C m}^{-2}$ ),  
soil total organic carbon ( $\text{kg C m}^{-2}$ )

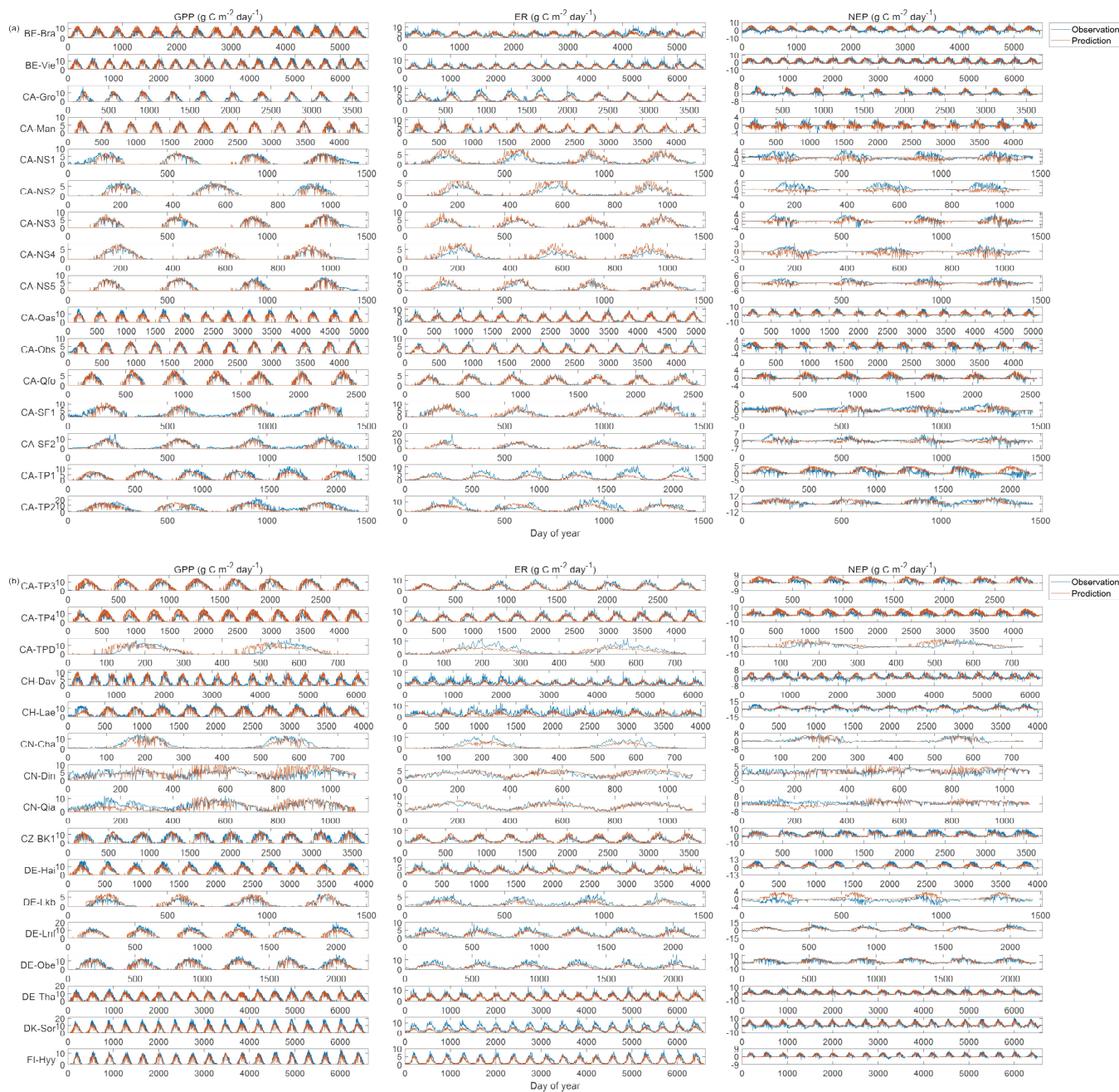
**Yearly:** same as the daily outputs, with the SOS dates  
(DOY) and EOS dates (DOY)

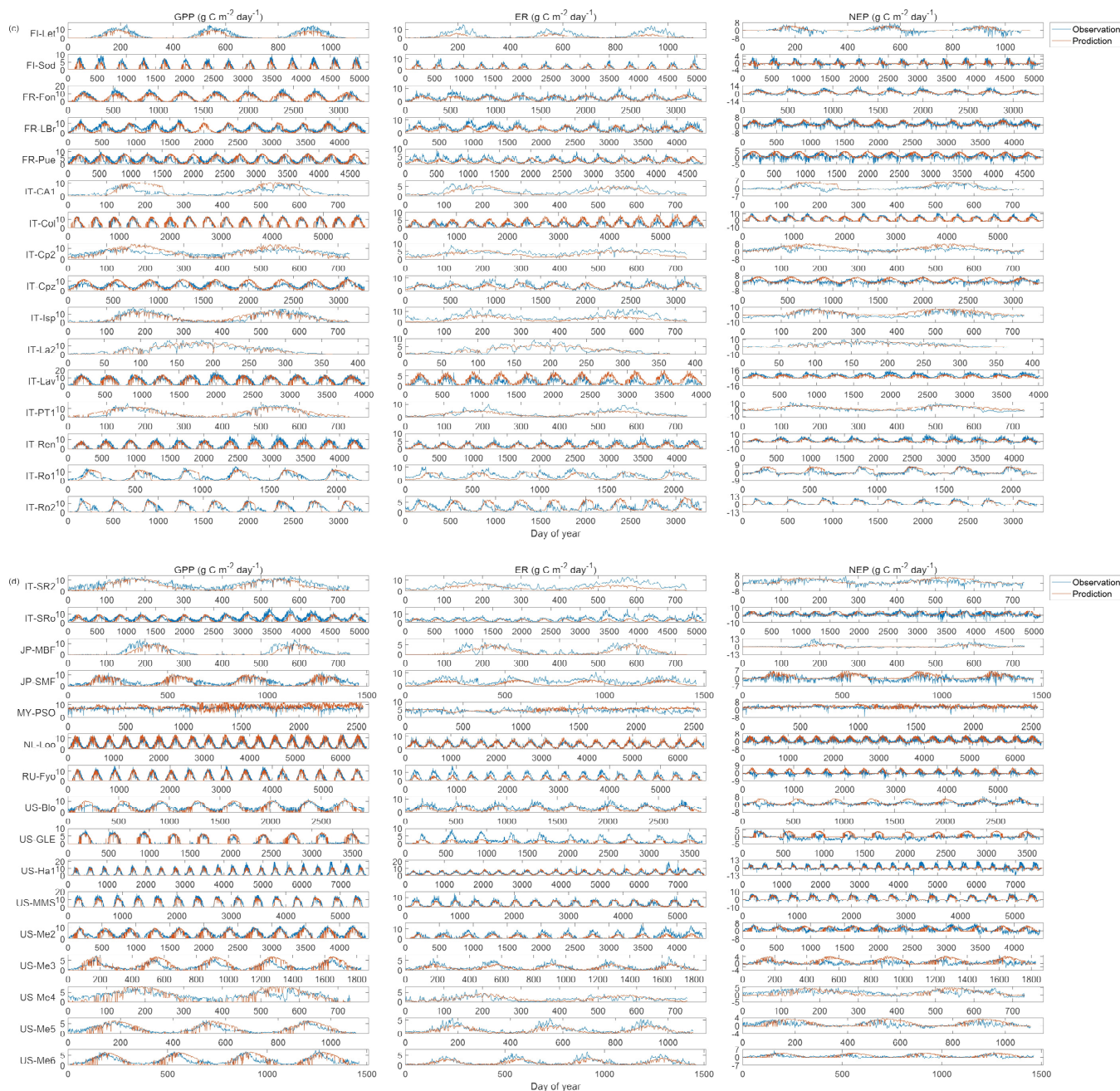
---





**Fig. 1.** Schematic representation of the FORCCHN2 model. LAI: leaf area index; NSC: non-structural carbohydrates; C: carbon; N: nitrogen.







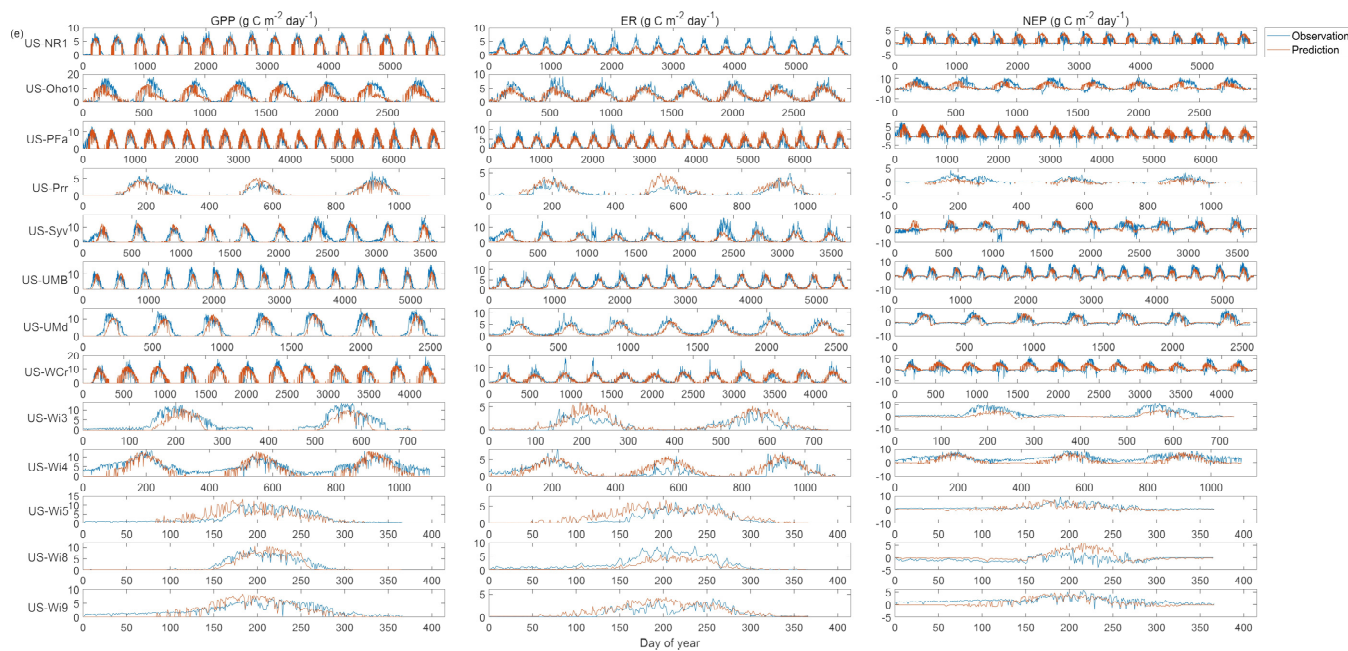


**Fig. 2.** The direct daily dynamic predictions and observations in the studied EC sites (the distribution and information of these sites can be found in Fig. S1 and Table S1). GPP: Gross Primary Productivity; ER: Ecosystem Respiration; NEP: Net Ecosystem Productivity.

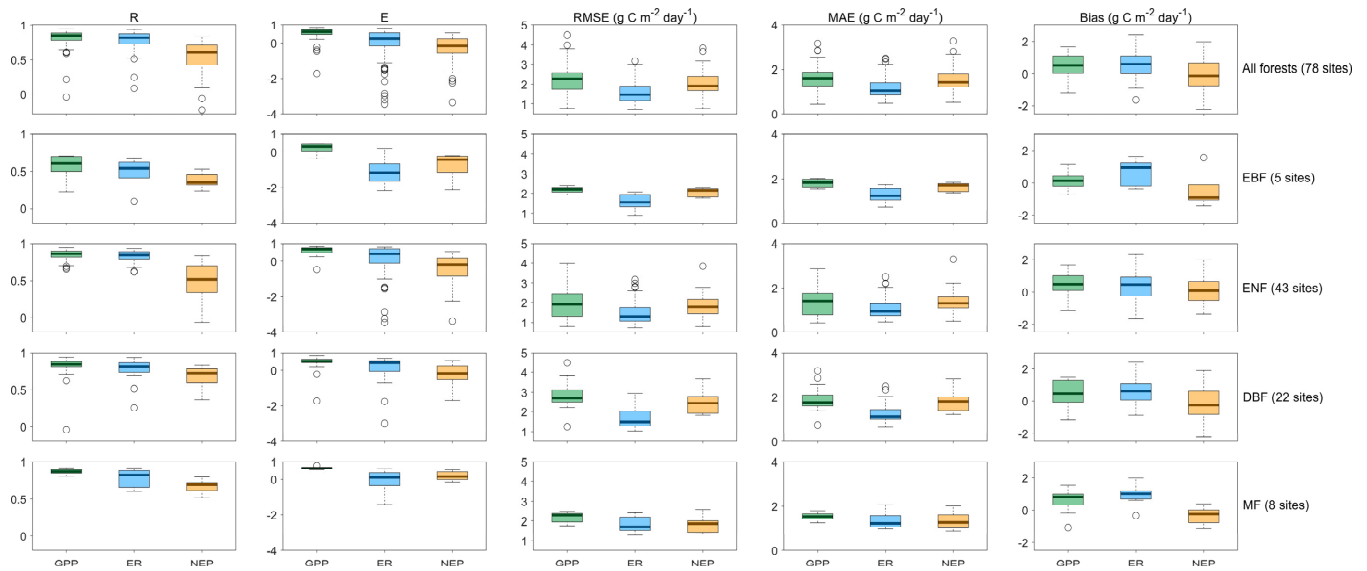


**Fig. 3.** The statistical results of daily gross primary productivity (GPP), ecosystem respiration (ER), and net ecosystem productivity (NEP) observations versus predictions in the studied EC sites. R: correlation coefficient; E: model efficiency; RMSE: root mean square error; MAE: mean absolute error; Bias: bias.

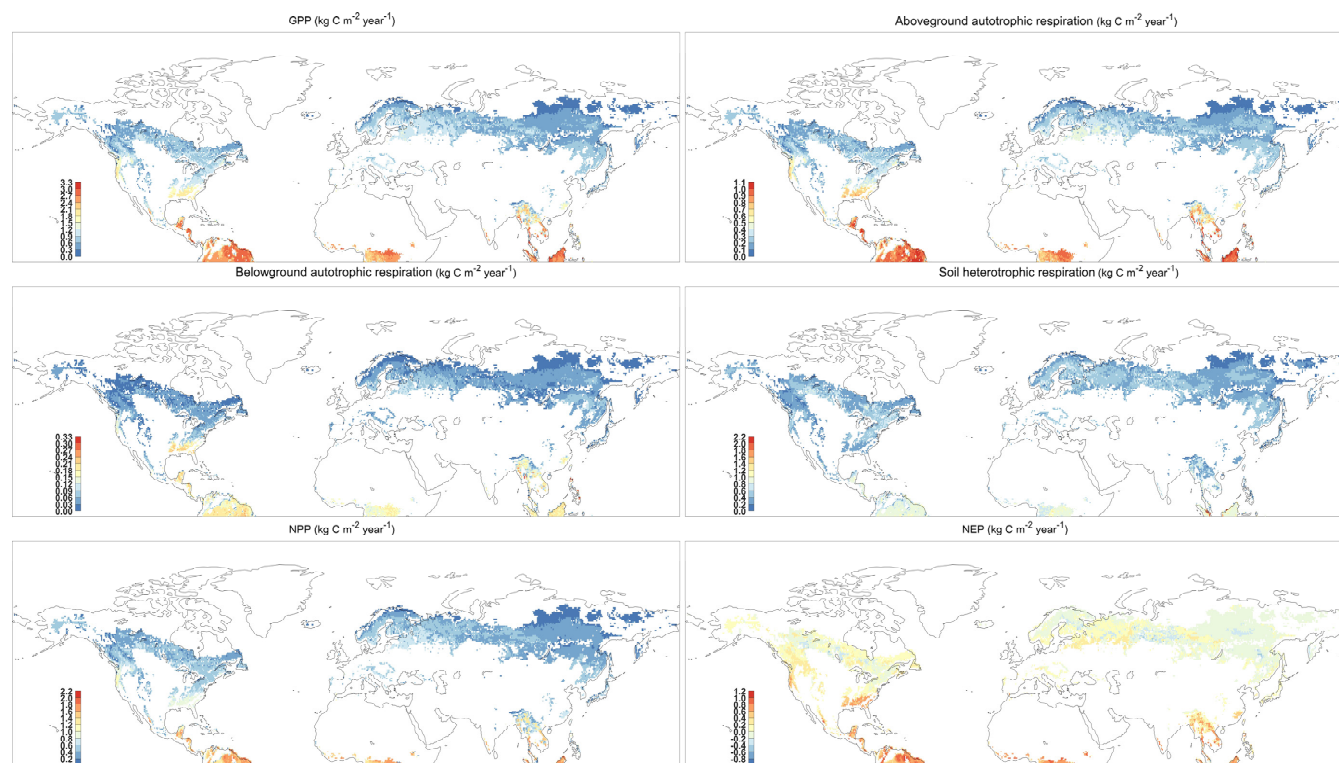


**Fig. 4.** The spatial distribution of mean GPP (Gross Primary Productivity), above- and belowground autotrophic respiration, soil heterotrophic respiration, NPP (Net Primary Productivity), and NEP (Net Ecosystem Productivity) predicted by the FORCCHN2 model for forest ecosystems of the Northern Hemisphere during 1980–2016. The spatial resolution is  $0.5^\circ \times 0.5^\circ$ .